A Study of the O^{4+} Emissivity Profiles with Two Separate Photon Emissivity Coefficient Databases and a Comparison of the Impurity Diffusion Coefficients in the Aditya Tokamak

Amrita BHATTACHARYA, Joydeep GHOSH[1], Malay B. CHOWDHURI[1], Prabhat MUNSHI, Izumi MURAKAMI[2] and the ADITYA team[1]

Nuclear Engineering and Technology Programme, Indian Institute of Technology Kanpur,
Kanpur-208016, Uttar Pradesh, India
[1]*Spectroscopy Diagnostic Division, Institute for Plasma Research, Gandhinagar, Bhat-382428, Gujarat, India*
[2]*National Institute for Fusion Science, Toki, Gifu 509-5292, Japan*

The present study is an analysis between radial emissivity profiles of the 650.024 nm transition of the O^{4+} ion obtained using two separate Photon Emissivity Coefficient (PEC) databases. Emissivity values of the 650.024 nm O^{4+} transition in visible-spectral region have been experimentally obtained for the Aditya tokamak. The radial number density distributions of different charge states of oxygen are estimated using a semi-implicit numerical method applied over the radial impurity transport equation. The 650.024 nm emissivity is calculated using the obtained impurity number density and with PECs from two separate databases namely the ADAS (Atomic Data and Analysis Structure) and the NIFS (National Institute for Fusion Science) database. Although impurity diffusivity profiles must not be dependent upon the choice of PEC databases; yet a requirement of separate impurity (oxygen) diffusivity profiles for the two PEC databases is observed, such that their corresponding calculated O^{4+} emissivities best depict the experimental emissivity data. A difference in the ionization and recombination rate coefficients provided in the ADAS and NIFS databases can lead to discrepancies in the impurity number densities calculated. The effects upon the impurity diffusivity while using ionization and recombination rate coefficients from two separate databases are further studied.

1. Introduction

Impurity ions while travelling from the plasma periphery towards the core very often collide with the electrons, main ions and amongst themselves. The impurity ions during such collisions can undergo one of the three phenomena namely excitation, ionization/ recombination and charge exchange based on the number density distribution of the colliding particles and the plasma temperature in the immediate region of collision. The ions, during any of the three processes, undergo a transition from its metastable state to ground state and in the process emit certain characteristic radiation. The radiations emitted are responsible for power loss and fuel dilution (in case of high Z impurities) in the plasma [1–4]. A given impurity distribution in tokamak is hence determined by means of spectrometers calibrated to measure its characteristic transition along several lines of sight such that the complete plasma cross-section is covered. Each signal obtained from the detectors is hence an integrated data over a given line of sight. The emissivity of the characteristic transition of an impurity ion is determined by means of inversion algorithms over the measured data [5–7].

The present study is a comparison between the experimental emissivity data and the calculated (simulated) emissivity values in the Aditya tokamak. The plasma in Aditya tokamak (minor radius $r_o = 0.25$ m, major radius $R = 0.75$ m, toroidal magnetic field $B_t = 0.75$ T) at the Institute for Plasma Research Gandhinagar, India is hydrogenic, confined within a graphite limiter and is circular in cross-section [8]. Experiment has been conducted to study the Be-like O^{4+} ion transport in Aditya tokamak using emissivity values of its characteristic 650.024 nm ($2p3p^3D_3$ - $2p3d^3F_4$) transition. The details of the experimental set-up used and the emissivity values obtained from the measured chord-integrated brightness using an Abel-like matrix inversion have been reported by M.B. Chowdhuri *et al.*[9]. The radial impurity transport equation for determining the impurity distribution in tokamak plasma is given as [10–13]:

$$\frac{\partial n_z(r,t)}{\partial t} = \frac{1}{r}\frac{\partial}{\partial r}\left[r\left(D(r)\frac{\partial n_z(r,t)}{\partial r} - v(r)\,n_z(r,t)\right)\right]$$
$$+ Q_z(r,t). \tag{1a}$$

The terms D and v represent diffusivity (m²/s) and convective velocity (m/s) of the impurity ion. The term Q_z in Eq. (1a) is described further as:

$$Q_z(r,t) = n_e(r)\,n_{z-1}(r,t)\,S_{z-1}(r)$$
$$- n_e(r)\,n_z(r,t)\,S_z(r)$$
$$+ n_e(r)\,n_{z+1}(r,t)\,\alpha_{z+1}(r)$$
$$- n_e(r)\,n_z(r,t)\,\alpha_z(r). \tag{1b}$$

The terms n_z, n_{z-1} and n_{z+1} represent the number densities (m⁻³) of Z, Z − 1 and Z + 1 impurity charge states respectively. The number density of electrons is represented as n_e (m⁻³). The terms S_z and S_{z-1} (m³/s) in Eq. (1b) are the ionization rate coefficients of Z and Z − 1 charge states of an impurity species and parameters α_z and α_{z+1} (m³/s) represent the recombination rate coefficients of impurity ions with charge states Z and Z + 1 respectively. The term r represents the plasma radius (m) and t represents the time (s). The initial condition for solving Eqs. (1a) - (1b) is given as:

$$n_z|_{t=0} = 0, \text{ for all } r \in [0,r_0]. \tag{1c}$$

The boundary conditions are given as:

a) $\left.\dfrac{dn_z}{dr}\right|_{r=r_o} = -\dfrac{n_z}{l_d}$, for all $0 \le t \le t_s$, $\qquad$ (1d)

b) $\left.\dfrac{dn_z}{dr}\right|_{r=0} = 0$, for all $0 \le t \le t_s$. $\qquad$ (1e)

The term l_d in Eq. (1d) represents the decay length (m) and the term t_s in Eq. (1e) represents the time at which steady state is attained. The calculated emissivity profiles are obtained by solving the radial impurity transport equation using a newly suggested semi-implicit numerical method [14] along with the Photon Emissivity Coefficients (PECs) from a given PEC database. The calculations in the present study have been performed in MATLAB® (The MathWorks Inc., Natick, MA, USA) using the High Performance Computing (HPC) facility [15] at the Indian Institute of Technology Kanpur, India. SI units have been followed throughout the study.

2. Theory

The detailed description of the semi-implicit numerical method recently applied over the radial impurity transport equation has been reported by Bhattacharya *et al.* [14]. The derivatives in the non-conservative formulation of the parabolic, coupled, radial impurity transport equation are primarily discretized by means of forward-differencing in time and central-difference scheme in space. The diffusivity terms after discretization and the ionization and recombination terms of charge state Z in Q_z (Eq. (1b)) are

subsequently rendered implicit. The terms associated with convective velocity, ionization of charge state Z − 1 and recombination of charge state Z+1 in Q_z remain explicit. The reason for treating the constituent terms after discretization as either implicit or explicit with respect to time has been reported in the aforementioned study [14]. The final linearized form of Eqs. (1a) - (1b) on applying the suggested semi-implicit method is expressed as:

$$\Delta t\left\{\frac{D_k}{(\Delta r)^2} + \frac{D_{k+1}}{4(\Delta r)^2} - \frac{D_{k-1}}{4(\Delta r)^2} + \frac{D_k}{2r_k\Delta r}\right\}n_z|_{k+1}^{j+1}$$
$$- \left\{1 + \frac{2D_k\Delta t}{(\Delta r)^2} + n_{e,k}S_{z,k}\Delta t + n_{e,k}\alpha_{z,k}\Delta t\right\}n_z|_k^{j+1}$$
$$+ \Delta t\left\{\frac{D_k}{(\Delta r)^2} - \frac{D_{k+1}}{4(\Delta r)^2} + \frac{D_{k-1}}{4(\Delta r)^2} - \frac{D_k}{2r_k\Delta r}\right\}n_z|_{k-1}^{j+1}$$
$$= \frac{v_k}{2\Delta r}\Delta t\, n_z|_{k+1}^{j} - \left\{1 + \Delta t\left[\frac{v_{k-1}}{2\Delta r} - \frac{v_k}{r_k} - \frac{v_{k+1}}{2\Delta r}\right]\right\}n_z|_k^{j}$$
$$- \frac{v_k}{2\Delta r}\Delta t\, n_z|_{k-1}^{j} - n_{e,k}\, n_{z-1}|_k^{j}\, S_{z-1,k}\Delta t$$
$$- n_{e,k}\, n_{z+1}|_k^{j}\, \alpha_{z+1,k}\,\Delta t. \tag{2}$$

The subscript k and superscript j in Eq. (2) represent the space and time iterations respectively. The suggested numerical scheme has been applied over the radial impurity transport equation in the region $0 < r < r_o$. The boundary conditions given in Eqs. (1d) - (1e) are solved as described in Eqs. (3a) - (3c).

Equation (1d) for $0 \le t \le t_s$ at the plasma edge $r = r_o$ is solved using a 3 point upwind scheme as follows:

$$\frac{3n_z|_{r=r_o} - 4n_z|_{r=r_o-\Delta r} + n_z|_{r=r_o-2\Delta r}}{2\Delta r} = -\frac{n_z|_{r=r_o}}{l_d} \tag{3a}$$

$$\Rightarrow \left\{n_z|_{r=r_o} - \frac{4}{\left(3 + \frac{2\Delta r}{l_d}\right)}n_z|_{r=r_o-\Delta r}\right.$$
$$\left. + \frac{1}{\left(3 + \frac{2\Delta r}{l_d}\right)}n_z|_{r=r_o-2\Delta r}\right\} = 0. \tag{3b}$$

Equation (1e) for $0 \le t \le t_s$ at the plasma centre (r = 0) is solved as follows:

$$(n_z|_{r=0} - n_z|_{r=\Delta r}) = 0. \tag{3c}$$

The radial emissivity profiles (ph m⁻³ s⁻¹ sr⁻¹) [16,17] of a given impurity ion with charge state Z is obtained using the equation:

$$E_z(r) = \frac{\begin{aligned}&n_e(r)\,n_{z,g}(r,t=t_s)\,\text{PEC}_z^{exc}(r)\\&+ n_e(r)\,n_{z+1,g}(r,t=t_s)\,\text{PEC}_{z+1}^{rec}(r)\\&+ n_H(r)\,n_{z+1,g}(r,t=t_s)\,\text{PEC}_{z+1}^{cx}(r)\end{aligned}}{4\pi}. \tag{4}$$

The charge state $Z = 1, 2, 3\dots, 8$ for oxygen.

The ground state (g) number densities $n_{z,g}$ and $n_{z+1,g}$ of a given impurity species are obtained by solving Eq. (2). The superscripts exc, rec and cx over the PECs (ph m³ s⁻¹) in Eq. (4) represent excitation, recombination and charge-exchange respectively. The parameter n_H represents the

Table 1   Experimental emissivity data of the 650.024 nm characteristic transition of O^{4+} ion along outboard (low magnetic field) region of Aditya plasma.

Left Bound $\rho - \Delta\rho$	ρ	Right Bound $\rho + \Delta\rho$	Experiment $E_{exp, out}$	Lower bound $E_{exp, out} - \Delta E_{exp}$	Upper bound $E_{exp, out} + \Delta E_{exp}$
-	-	-	(ph m^{-3} sr^{-1} s^{-1})	(ph m^{-3} sr^{-1} s^{-1})	(ph m^{-3} sr^{-1} s^{-1})
0.858	0.928	0.998	8.868E+16	7.537E+16	1.020E+17
0.726	0.796	0.866	1.344E+17	1.142E+17	1.545E+17
0.594	0.664	0.734	3.907E+17	3.321E+17	4.493E+17
0.462	0.532	0.602	9.941E+16	8.450E+16	1.143E+17

number density of hydrogen ion in Aditya plasma. The present study compares the O^{4+} emissivity profiles of its characteristic 650.024 nm (2p3p^{3}D$_3$ - 2p3d^{3}F$_4$) transition in the visible spectral region with the experimental emissivity data. The experimental emissivity data in the outboard (low-magnetic field) region of Aditya tokamak is only considered. The Photon Emissivity Coefficients for the calculated emissivity profiles are obtained from two separate databases namely the ADAS (Atomic Data and Analysis Structure) and the NIFS (National Institute for Fusion Science) database. Emissions from O^{4+} ions only due to excitation are however considered in the present study based on the temperature profile of Aditya tokamak and absence of any neutral beam heating in the same. The first term only in Eq. (4) is hence considered.

3.   Results and Discussions

Emissivity values of the characteristic 650.024 nm transition of O^{4+} ion in visible-spectral region, based on the experimental measurements in Aditya tokamak, are described in Table 1. Four of the radial points of measurement that lie between $0.50 \geq \rho \geq 0.95$ (Region of Interest ROI-outboard) in Aditya plasma have been considered. Table 1 reports the experiment emissivity data $E_{exp, out}$, along with their lower and upper ordinate bounds. An uncertainty of maximum 15% associated with each experimental data has been reported by Chowdhuri et al. [9]. The left and right abscissa bounds are considered as $\Delta\rho = \pm 0.07$ ($\Delta r = \pm 0.0175$ m) in the present study.

The Gaussian function E_{Gauss} shown in Eq. (5) has been generated to fit the experiment emissivity data which would best describe the trend of O^{4+} (650.024 nm) emissivity at all radii in the outboard section of Aditya plasma.

$$E_{Gauss}(\rho) =$$
$$E_{Gauss, peak} \frac{1}{\sqrt{2\pi\sigma_1^2}} \exp\left(\frac{-[\rho - 0.690]^2}{2\sigma_1^2}\right). \qquad (5)$$

The terms $E_{Gauss, peak} = 1.0E+17$ ph m^{-3} sr^{-1} s^{-1} and $\sigma_1 = 0.098$ in Eq. (5). The E_{Gauss} profile has been obtained with mesh size $\Delta r = 2E-03$ m. The radial profiles

of the input parameters to the applied semi-implicit numerical method, namely number density of electron (n_e), plasma temperature (T_e) and the neutral oxygen number density ($O_{neutral}$) are shown in Figs. 1 (a) - (c) respectively. The n_e, T_e, and $O_{neutral}$ profiles in Figs. 1(a) - (c) have been modelled as:

$$T_e(r) = T_{e,a} + (T_{e,0} - T_{e,a})\left[1 - \left(\frac{r}{r_o}\right)^2\right]^a, \qquad (6a)$$

$$n_e(r) = n_{e,a} + (n_{e,0} - n_{e,a})\left[1 - \left(\frac{r}{r_o}\right)^2\right]^b, \qquad (6b)$$

$$O_0(r) = O_{0, peak} \exp\left[-\left(\frac{r_o - r}{2\pi\frac{r_o}{\gamma}}\right)^{2.65}\right]. \qquad (6c)$$

The values of various terms used in Eqs. (6a) - (6b) are as follows: $T_{e,0} = 350$ eV, $T_{e,a} = 12.5$ eV, $n_{e,0} = 2.0E+19$ m^{-3}, $n_{e,a} = 2.3E+18$ m^{-3}. These values are typical parameters for the Aditya tokamak discharges. The radial profile of the electron number density (n_e) is obtained by Abel inverting the chord integrated data from seven-channel microwave interferometer. The radial profile of the electron temperature (T_e) is reconstructed based on measured values of the central temperature from Soft X-Ray (SXR) intensity ratio and the edge temperature from Langmuir probes and spectroscopy. The n_e and T_e measurements in the Aditya tokamak have been described in details by Chowdhuri et al. [9] and Dey et al. [16]. Based on the nature of the measured profiles, the values a = b = 1.32, in Eqs. (6a) and (6b) have been considered in the present study. The oxygen impurity concentration and the radial profile of impurity diffusion coefficient are obtained by iteratively constraining the simulated radial emissivity profile to the experimentally measured emissivity data of the 650.024 nm characteristic transition of O^{4+} ion in Aditya tokamak. The radial profile of $O_{neutral}$, once validated, have been maintained the same for all further calculations in the present study. The values of $O_{0, peak} = 9.40E+16$ m^{-3} (i.e. O_0 (r) at r = r_o) and $\gamma = 39.8$ respectively have been considered in Eq. (6c). The effective ionization and effective recombination rate coefficients of the oxygen ions obtained from the Atomic Data and Structure Analysis ADAS
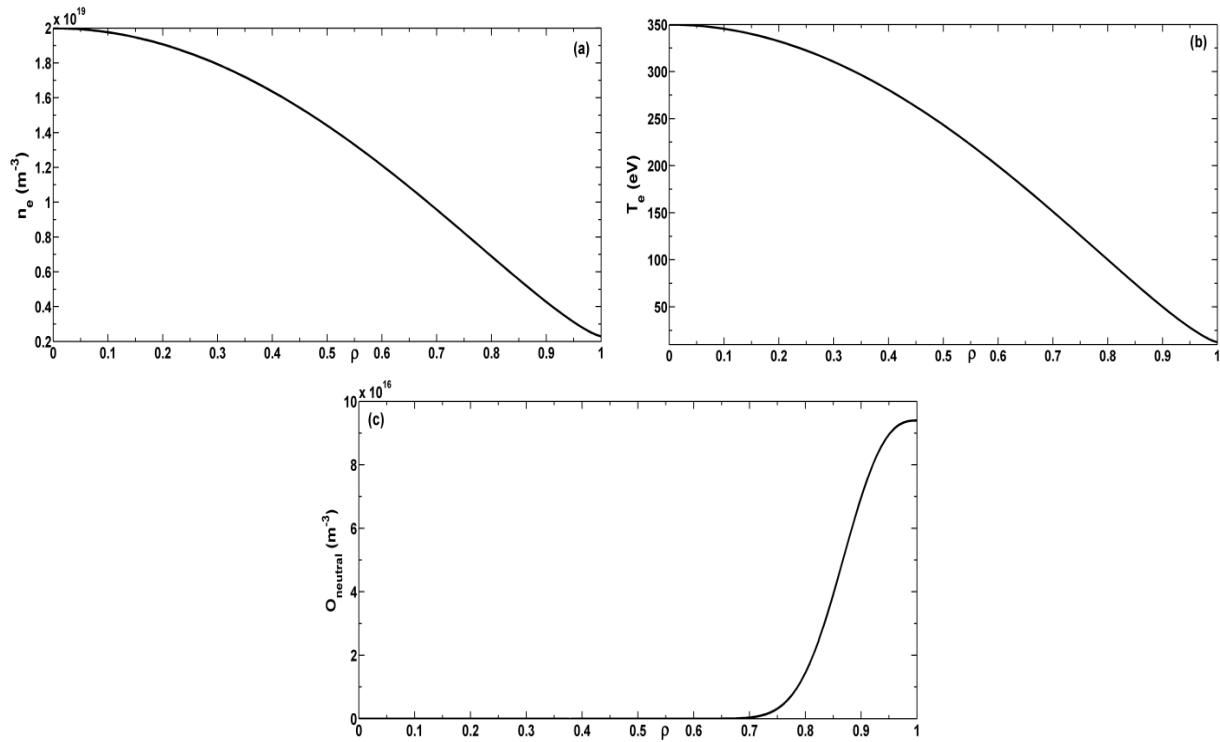
Fig. 1 Profiles of (a) electron number density n_e (m^{-3}), (b) plasma temperature T_e (eV), (c) neutral oxygen number density $O_{neutral}$ (m^{-3}) with respect to normalized plasma radius ρ.

database [18] are interpolated based on the temperature and electron number density profile of the Aditya tokamak (Fig. 1).

The radial profile of impurity diffusion coefficient has been modelled as follows [19]:

$$\text{If } r > r_m, \ D(r) = D_a + (D_m - D_a) \exp\left[\frac{-(r - r_m)^2}{p_1^2}\right]$$

$$\text{If } r < r_m, \ D(r) = D_0 + (D_m - D_0) \exp\left[\frac{-(r - r_m)^2}{p_2^2}\right].$$

(6d)

The values of various terms in Eq. (6d) are as follows: $r_o = r_{LCFS} = 0.25\,\text{m}$; $D_0 = 3.0\,\text{m}^2/\text{s}$; $D_m = 31.0\,\text{m}^2/\text{s}$; $D_a = 52.0\,\text{m}^2/\text{s}$; $p_1 = 6.0\text{E-}02\,\text{m}$; $p_2 = 2.0\text{E-}02\,\text{m}$; $p_m = 0.605$ and $r_m = p_m \times r_{LCFS} = 0.1513\,\text{m}$ respectively. The radial profile of the diffusion coefficient, with the values of all its terms in Eq. (6d), is considered to be same for all oxygen ions while computing their number densities using the semi-implicit radial impurity transport equation. The impurity diffusion coefficients in classical and Pfirsch-Schlüter regimes of neo-classical transport do not depend on the impurity charge state Z [13] when the main ion collisionality is low. The impurity diffusion coefficient in the Banana-Plateau regime of neo-classical theory is predicted to be a weak function of the impurity collisionality and a decreasing function of the impurity charge state Z [20]. Further, the turbulent diffusion coefficient corresponding to the random walk of every particle about the fluctuating potential, with the $\overrightarrow{E} \times \overrightarrow{B}$ drift

velocity $\overrightarrow{V_E} = \frac{\overrightarrow{E} \times \overrightarrow{B}}{B^2}$, is found to be independent of the particle charge state Z [21, 22]. Furthermore, experimental studies of the Z dependency of the impurity diffusion coefficients are found to be varying from machine to machine. A weak dependence on the impurity charge states is reported in the Large Helical Device (LHD) [23] whereas in ASDEX-U tokamak, it is found to be following the Z dependence as predicted neo-classically in Banana-Plateau regime [24]. The impurity diffusion coefficients driven by turbulence transport is mostly anomalous in nature and the parametric dependence on the impurity mass and charge is yet to be fully established, both theoretically and experimentally. Considering all of these facts, for relatively low density and low temperature plasma of Aditya tokamak, the assumption of Z independence of diffusion coefficient is fairly reasonable for number density calculations of different charge stages of oxygen. A radially constant value of the convective velocity v = 0.001 m/s has been considered that is assumed to remain same for all oxygen ions. The number density profiles of the oxygen ions using the aforementioned semi-implicit method are obtained with a mesh size $\Delta r = 2\text{E-}03\,\text{m}$ and time step $\Delta t = 7.5\text{E-}09\,\text{s}$. The emissivity profiles of the characteristic 650.024 nm transition are determined using number density of O^{4+} ion, obtained by solving the radial impurity transport equation using the semi-implicit numerical method (Eq. (2)), along with the Photon Emissivity Coefficients from the ADAS [25] and NIFS databases (Eq. (4)). The various parameters in the equation for obtaining the
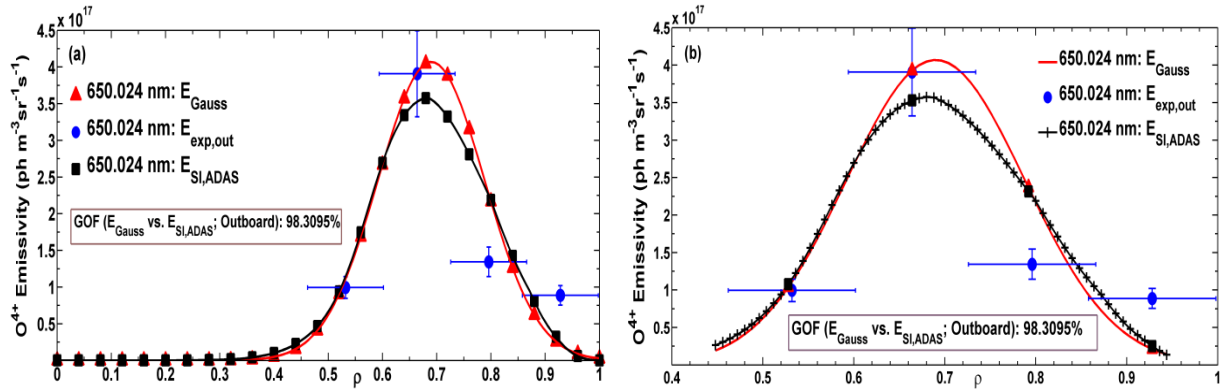
Fig. 2 Experimental emissivity data, Gaussian emissivity model and the calculated (semi-implicit) emissivity for (a) outboard section, (b) ROI-outboard of Aditya plasma with respect to normalized radius ρ for 650.024 nm transition of O^{4+} ion with PECs from the ADAS database.

Table 2 Comparison between the experimental, modelled (Gaussian) and calculated (semi-implicit) emissivity of O^{4+} ion (650.024 nm transition) with PEC-ADAS at four radial points of measurement in the outboard section of Aditya plasma.

ρ	$E_{exp,\,out}$	ρ_{cal}	E_{Gauss}	% deviation	$E_{SI,\,ADAS}$	% deviation
-	(ph m^{-3} sr^{-1} s^{-1})	-	(ph m^{-3} sr^{-1} s^{-1})	-	(ph m^{-3} sr^{-1} s^{-1})	-
0.928	8.868E+16	0.928	2.133E+16	75.95%	2.515E+16	71.63%
0.796	1.344E+17	0.792	2.368E+17	76.26%	2.315E+17	72.32%
0.664	3.907E+17	0.664	3.930E+17	0.58%	3.530E+17	9.66%
0.532	9.941E+16	0.528	1.038E+17	4.44%	1.076E+17	8.24%

radial diffusion coefficient profile (Eq. (6d)) were varied iteratively to obtain the best match between the simulated (Eqs. (2) and (4)) and Gaussian (Eq. (5)) emissivity profiles and the experimentally measured O^{4+} (650.024 nm) emissivity data in Aditya tokamak. The impurity diffusion coefficient and impurity concentration corresponding to the 'best-fit' simulated (semi-implicit transport equation) 650.024 nm O^{4+} emissivity profiles are treated as the outcome of the modelling, used for understanding the oxygen transport in Aditya tokamak.

Figures 2 (a), (b) describe the experimental data $E_{exp,\,out}$, the modelled Gaussian emissivity profile E_{Gauss} and the calculated (semi-implicit) emissivity profile $E_{SI,\,ADAS}$ of the 650.024 nm transition of O^{4+} ion. The figures show the 'Goodness of Fit' between the E_{Gauss} and $E_{SI,\,ADAS}$ profile is 98.31% thereby attesting that the two profiles are in 'good agreement' with each other and with the experimental data as further enunciated in Table 2.

Table 2 compares these O^{4+} (650.024 nm) emissivity values at the four radial (ρ) points of experimental measurement. The term ρ_{cal} in Table 2 represents the normalized radius (closest to the experimental ρ) with mesh size $\Delta r = 0.002$ m corresponding to which E_{Gauss} and $E_{SI,\,ADAS}$ have been reported in the table. The % deviation reported in Table 2 is the deviation of E_{Gauss} or $E_{SI,\,ADAS}$ emissivities
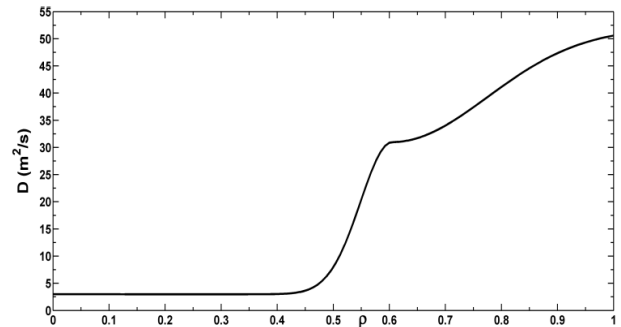

Fig. 3 The impurity diffusion coefficient D (m^2/s) with respect to normalized plasma radius ρ corresponding to the 'best-fit' calculated 650.024 nm emissivity profile with O^{4+} (simulated) number density and PEC-ADAS in Aditya tokamak.

with respect to the experimental emissivity data $E_{exp,\,out}$.

The impurity diffusion coefficient obtained using Eq. (6d) corresponding to the best-fit emissivity profile, calculated with the O^{4+} number density (semi-implicit method) and the PEC-ADAS database (Fig. 2), is shown in Fig. 3. The impurity diffusion coefficient profile shown in Fig. 3 is similar to the diffusivity profile earlier reported
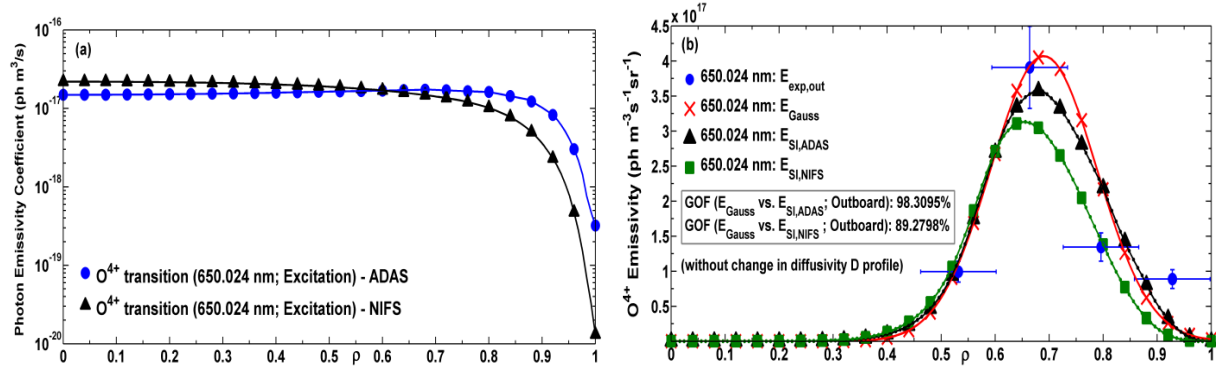
Fig. 4 (a) Photon Emissivity Coefficients (PEC) (650.024 nm excitation line) of ADAS and NIFS database with respect to normalized plasma radius ρ, (b) Experimental, Gaussian and Calculated O^{4+} emissivity (with PEC-ADAS and PEC-NIFS) of the 650.024 nm excitation line with respect to ρ with no change in D profile.

Table 3 Comparison between the experimental, modelled (Gaussian) and calculated (semi-implicit) emissivity of O^{4+} ion (650.024 nm transition) with PEC-NIFS at four radial points of measurement in the outboard section of Aditya plasma (w/o change in D).

ρ	$E_{exp, out}$	ρ_{cal}	E_{Gauss}	% deviation	$E_{SI, NIFS}$	% deviation
-	(ph m^{-3} sr^{-1} s^{-1})	-	(ph m^{-3} sr^{-1} s^{-1})	-	(ph m^{-3} sr^{-1} s^{-1})	-
0.928	8.868E+16	0.928	2.133E+16	75.95%	6.525E+15	92.64%
0.796	1.344E+17	0.792	2.368E+17	76.26%	1.507E+17	12.18%
0.664	3.907E+17	0.664	3.930E+17	0.58%	3.117E+17	20.22%
0.532	9.941E+16	0.528	1.038E+17	4.44%	1.200E+17	20.69%

for the outboard section of Aditya plasma by Chowdhuri *et al.* [9].

3.1 Comparison between the 650.024 nm O^{4+} emissivity obtained using two separate PEC databases

A second Photon Emissivity Coefficient (PEC) database used for determining the O^{4+} emissivity profile (650.024 nm) is the database from the National Institute for Fusion Science (NIFS), Japan. Figure 4 (a) shows a comparison between the Photon Emissivity Coefficient (PEC) profiles, for the 650.024 nm transition of O^{4+} ion, corresponding to the ADAS [25] and NIFS database. Figure 4 (b) describes the experimental data $E_{exp, out}$, the modelled Gaussian emissivity profile E_{Gauss}, the calculated (semi-implicit) emissivity profile $E_{SI, ADAS}$ using the PEC-ADAS database and the calculated (semi-implicit) emissivity profile $E_{SI, NIFS}$ using the PEC-NIFS database respectively for the 650.024 nm transition of O^{4+} ion. The O^{4+} number density while calculating $E_{SI, NIFS}$ in Fig. 4 (b) is the same as used for calculating $E_{SI, ADAS}$ and only the PECs differ (Eq. (4)) while calculating the two emissivities. Figure 4 (b) shows the 'Goodness of Fit' between the Gaussian and the calculated emissivity profile using the PEC-NIFS is 89.28%.

Table 3 shows the experimental, Gaussian and calculated emissivity values using PEC-NIFS at the four radial points of measurement in the outboard section of Aditya plasma. The $E_{SI,NIFS}$ profile in Fig. 4 (b) along with its % deviation with respect to the experimental emissivity data in Table 3 shows the need for a different number density profile of O^{4+} ion based on which, using Eq. (4), a calculated emissivity profile using PEC-NIFS must be obtained that matches well with the Gaussian profile as well as with the experimental emissivity data.

A separate impurity diffusion coefficient profile shown in Fig. 5 (a), different from the ones applied in case of PEC-ADAS, is used for computing the required O^{4+} number density using the semi-implicit numerical method in case of the PEC-NIFS database (650.024 nm excitation transition). The input parameters to the applied semi-implicit numerical method, except the impurity diffusion coefficient profile, all remain same while calculating the number density of oxygen ions using the semi-implicit numerical method. The radial impurity transport equation using the semi-implicit method is solved with the mesh size Δr = 2E-03 m and time step Δt = 7.5E-09 s.

Figure 5 (a) compares between the oxygen ion diffusivity profiles used to calculate the O^{4+} number density using the semi-implicit numerical method corresponding to the PEC-ADAS and PEC-NIFS database. The im-
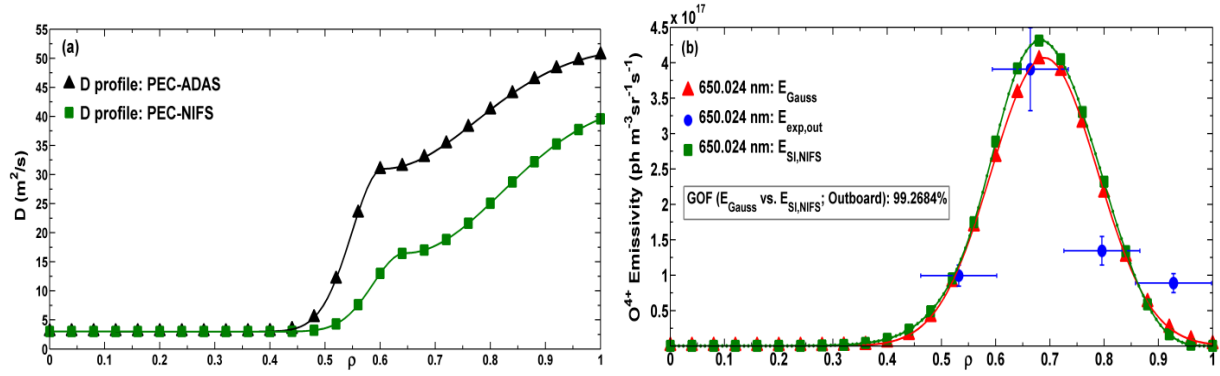
Fig. 5 (a) Separate profiles of impurity diffusivity D (m²/s) with respect to normalized plasma radius ρ corresponding to the ADAS and NIFS database, (b) Experimental, Gaussian and Calculated emissivity (with PEC-NIFS) of the 650.024 nm excitation line with respect to ρ based on the change in D profile.

Table 4 Comparison between the experimental, modelled (Gaussian) and calculated (semi-implicit) emissivity of O^{4+} ion (650.024 nm transition) with PEC-NIFS at four radial points of measurement in the outboard section of Aditya plasma (with change in D).

ρ	$E_{exp, out}$	ρ_{cal}	E_{Gauss}	% deviation	$E_{SI, NIFS}$	% deviation
-	(ph m^{-3} sr^{-1} s^{-1})	-	(ph m^{-3} sr^{-1} s^{-1})	-	(ph m^{-3} sr^{-1} s^{-1})	-
0.928	8.868E+16	0.928	2.133E+16	75.95%	1.185E+16	86.63%
0.796	1.344E+17	0.792	2.368E+17	76.26%	2.516E+17	87.24%
0.664	3.907E+17	0.664	3.930E+17	0.58%	4.242E+17	8.57%
0.532	9.941E+16	0.528	1.038E+17	4.44%	1.083E+17	8.90%

purity diffusivity, corresponding to PEC-NIFS, is determined using Eq. (6d) as well. The values of various terms in Eq. (6d) for the separate diffusivity are $r_o = r_{LCFS} = 0.25$ m; $D_0 = 3.0$ m²/s; $D_m = 16.5$ m²/s; $D_a = 43.0$ m²/s; $p_1 = 6.2E\text{-}02$ m; $p_2 = 2.05E\text{-}02$ m; $p_m = 0.645$ and $r_m = p_m \times r_{LCFS} = 0.1613$ m respectively. A comparison between the two diffusivity profiles in Fig. 5 (a) shows the trend of both profiles remain similar i.e. an increase in impurity diffusivity from the plasma core towards the edge is observed. The magnitude of the impurity diffusivity from the mid-plasma region till the edge is however lesser among the two in case of the PEC-NIFS database. The values of p_m in the two profiles i.e. $p_{m, ADAS} = 0.605$ and $p_{m, NIFS} = 0.645$ further suggests the step (mid) region of the diffusivity profile is more inclined towards the plasma edge in case of $D_{PEC-NIFS}$. The O^{4+} (650.024 nm) emissivity profile calculated using the O^{4+} number density, with a separate impurity diffusivity profile in case of PEC-NIFS database, is shown in Fig. 5 (b). The 'Goodness of Fit' between the calculated (PEC-NIFS) and the Gaussian emissivity is obtained as 99.27% in such case. The two emissivity profiles are hence found to be in good agreement with each other. Table 4 compares the O^{4+} (650.024 nm) emissivity, calculated using the separately obtained O^{4+} number density from the semi-implicit method and PECs from the NIFS database, with emissivity values from the Gaussian

model and the experimental emissivity data (outboard) at the four radial points of measurement.

Figures 6 (a), (b) summarizes the O^{4+} emissivity profiles of the 650.024 nm transition obtained through experiment, Gaussian model and calculated emissivities in case of PEC-ADAS and PEC-NIFS database, with separate diffusivity profiles in the two cases of emissivities numerically calculated. Table 5 further describes the emissivity values at the four radial points of measurement in the outboard section of Aditya plasma.

The nature of the impurity emissivity profiles should not be dependent upon the profiles of impurity transport coefficients used while calculating their number densities with radial impurity transport equation. The requirement of a separate diffusivity profile while calculating the O^{4+} emissivity in case of the PEC-NIFS data is attributed to the difference between the PEC coefficient profiles of the 650.024 nm O^{4+} transition obtained from the ADAS and NIFS database. The difference in the PEC profiles is more extensive (in orders of 10) towards the plasma edge than towards the plasma centre especially for $\rho \geq 0.6$ as seen in Fig. 4 (a). The O^{4+} ion distribution, on the other hand based on the Aditya parameters (Figs. 1 (a) - (c) & Fig. 3), is prominent in Aditya plasma beyond $\rho = 0.6$. The difference in the calculated O^{4+} emissivity profiles, hence based on Eq. (4), is also extensive beyond $\rho = 0.6$ (Fig. 4 (b))
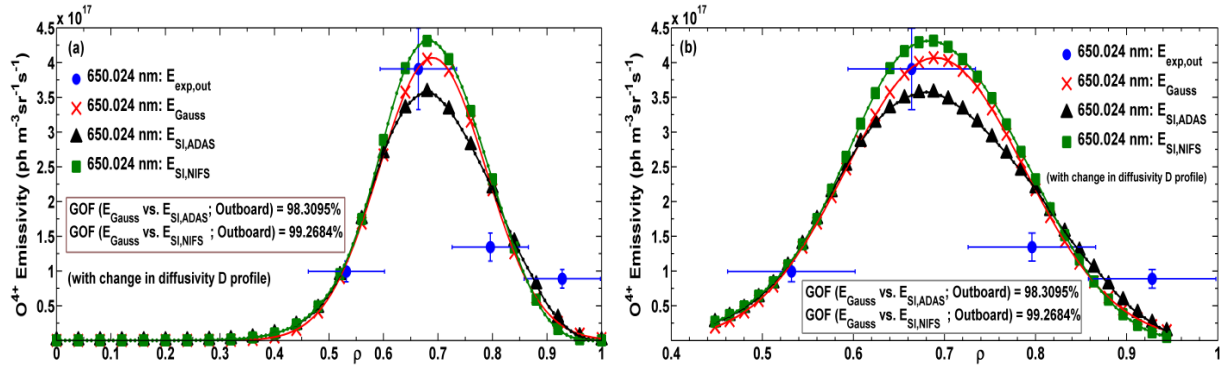
Fig. 6 Experimental emissivity data, Gaussian emissivity model and the calculated (semi-implicit) emissivity with PEC-ADAS and PEC-NIFS for (a) outboard section, (b) ROI-outboard of Aditya plasma with respect to normalized radius ρ for 650.024 nm transition of O^{4+} ion with PECs from the ADAS database.

Table 5 Comparison between the experimental, calculated (semi-implicit) emissivity with PEC-ADAS and calculated (semi-implicit) emissivity with PEC-NIFS of O^{4+} ion (650.024 nm transition) at four radial points of measurement in the outboard section of Aditya plasma (with change in D).

ρ	$E_{exp, out}$	ρ_{cal}	$E_{SI, ADAS}$	% deviation	$E_{SI, NIFS}$	% deviation
-	(ph m^{-3} sr^{-1} s^{-1})	-	(ph m^{-3} sr^{-1} s^{-1})	-	(ph m^{-3} sr^{-1} s^{-1})	-
0.928	8.868E+16	0.928	2.515E+16	71.63%	1.185E+16	86.63%
0.796	1.344E+17	0.792	2.315E+17	72.32%	2.516E+17	87.24%
0.664	3.907E+17	0.664	3.530E+17	9.66%	4.242E+17	8.57%
0.532	9.941E+16	0.528	1.076E+17	8.24%	1.083E+17	8.90%

pointing towards the need for a separate diffusivity profile. The difference in the PEC coefficient profiles shown in Fig. 4 (a) is due to a difference in the atomic and molecular processes considered while calculating the coefficients in the two databases. The direct transition from the ground state to the upper level in case of 650.024 nm excitation transition is forbidden and the excitation pass consists of two separate transitions. The excitation rate coefficients determining the PECs are different for the ADAS (CR model) and NIFS database based on the two different models applied in either case. A further study regarding the atomic processes considered while calculating the PEC coefficients in NIFS database is hence required.

3.2 Study of the ionization and recombination rate coefficients provided in the ADAS and NIFS database and the effect of their difference over the impurity number density

The emissivity due to a characteristic transition of an impurity ion is dependent upon its number density distribution in the plasma studied (Eq. (4)). The number density distribution of a given impurity species obtained is dependent upon the ionization and recombination rate coefficients of the ions with charge state Z, Z − 1 and Z + 1

respectively as described in Eq. (1b). A further study of the ionization and recombination rate coefficients of the oxygen ions (O^{1+} to O^{8+}) provided in the ADAS and NIFS database [26] is conducted based on the electron number density and plasma temperature profiles in the Aditya tokamak (Figs. 1 (a), (b)). Figures 7 (a) - (h) show the ionization rate coefficients of the oxygen ion obtained from the two databases using the Aditya plasma parameters. Figures 8 (a) - (h) show the recombination rate coefficients of the oxygen ion obtained from the two databases using the Aditya plasma parameters. The figures show a difference in the ionization and recombination rate coefficients obtained from the two databases that evidently effects the number density distribution of the oxygen ions while solving the radial impurity transport equation using the semi-implicit numerical method. Figures 9 (a) - (h) describe the difference in the number density distribution of oxygen ions as an effect of using the ionization (ion.) rate coefficient and recombination (rec.) rate coefficient data from the two separate databases.

The parameters as shown in Figs. 1 (a) - (c) and Fig. 3, while calculating the number densities of oxygen ions using the semi-implicit numerical method (Fig. 9), remain same for the ADAS and NIFS (ionization and recombination rate coefficient) databases. The mesh size and time step used for the semi-implicit numerical method in case
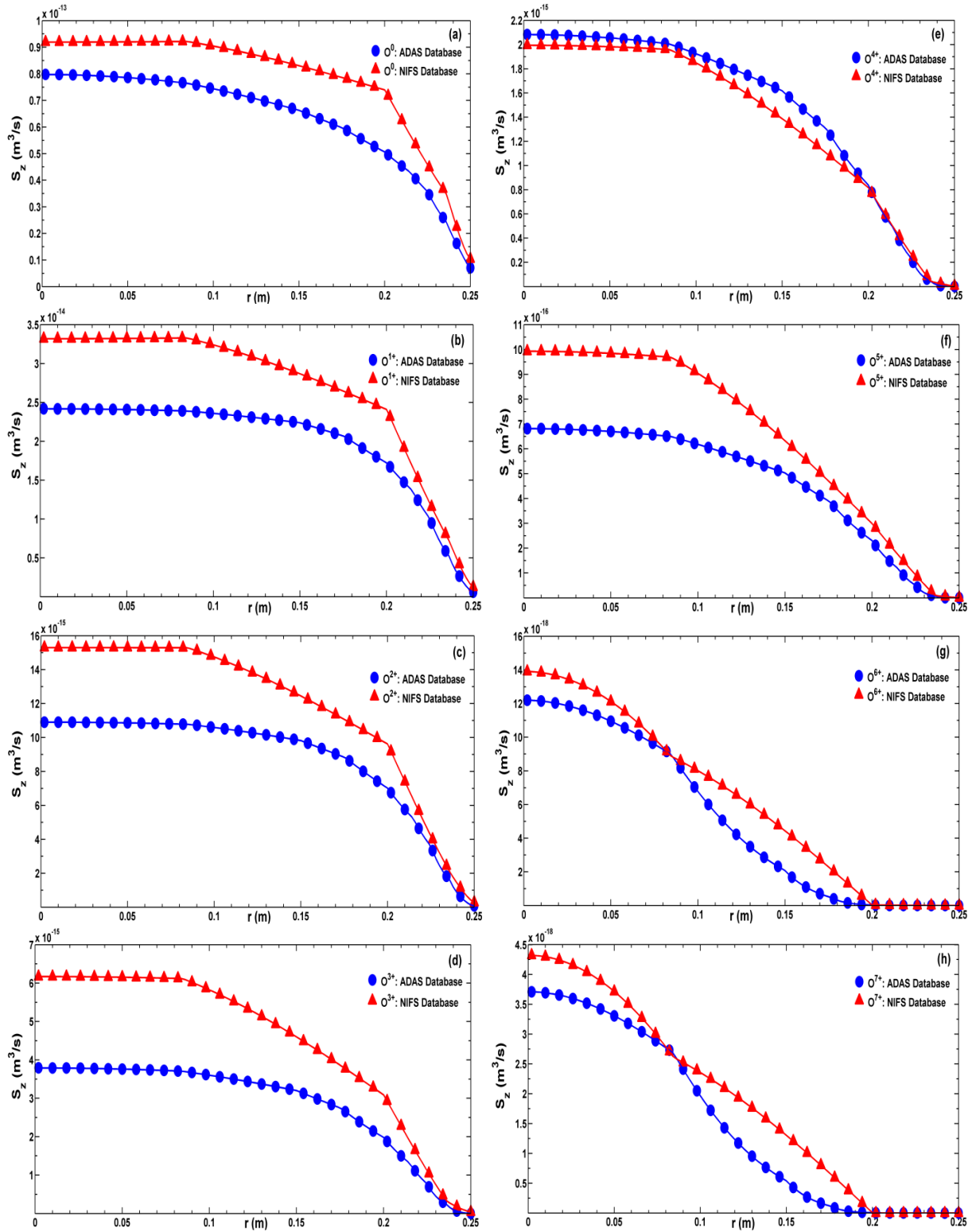
Fig. 7   Ionization Rate Coefficients S_z (m³/s) of (a) O^0, (b) O^{1+}, (c) O^{2+}, (d) O^{3+}, (e) O^{4+}, (f) O^{5+}, (g) O^{6+}, (h) O^{7+} ion with respect to radius r (m) from the ADAS and NIFS databases for the plasma parameters of Aditya tokamak.

of the NIFS (ION./REC.) data are Δr = 2E-03 m and Δt = 1.25E-08 s respectively. Table 6 further describes the % deviation in the peak value of the number densities of oxygen ions on using two separate databases of ionization and recombination rate coefficients namely the ADAS

and NIFS databases. The % deviations in the Table 6 along with Figs. 9 (a) - (h) show the number densities of the oxygen ions are in good agreement with each other. The difference in the rate coefficients obtained from the ADAS and NIFS databases (Figs. 7(a) - (h) and Figs. 8 (a) - (h)) seldom
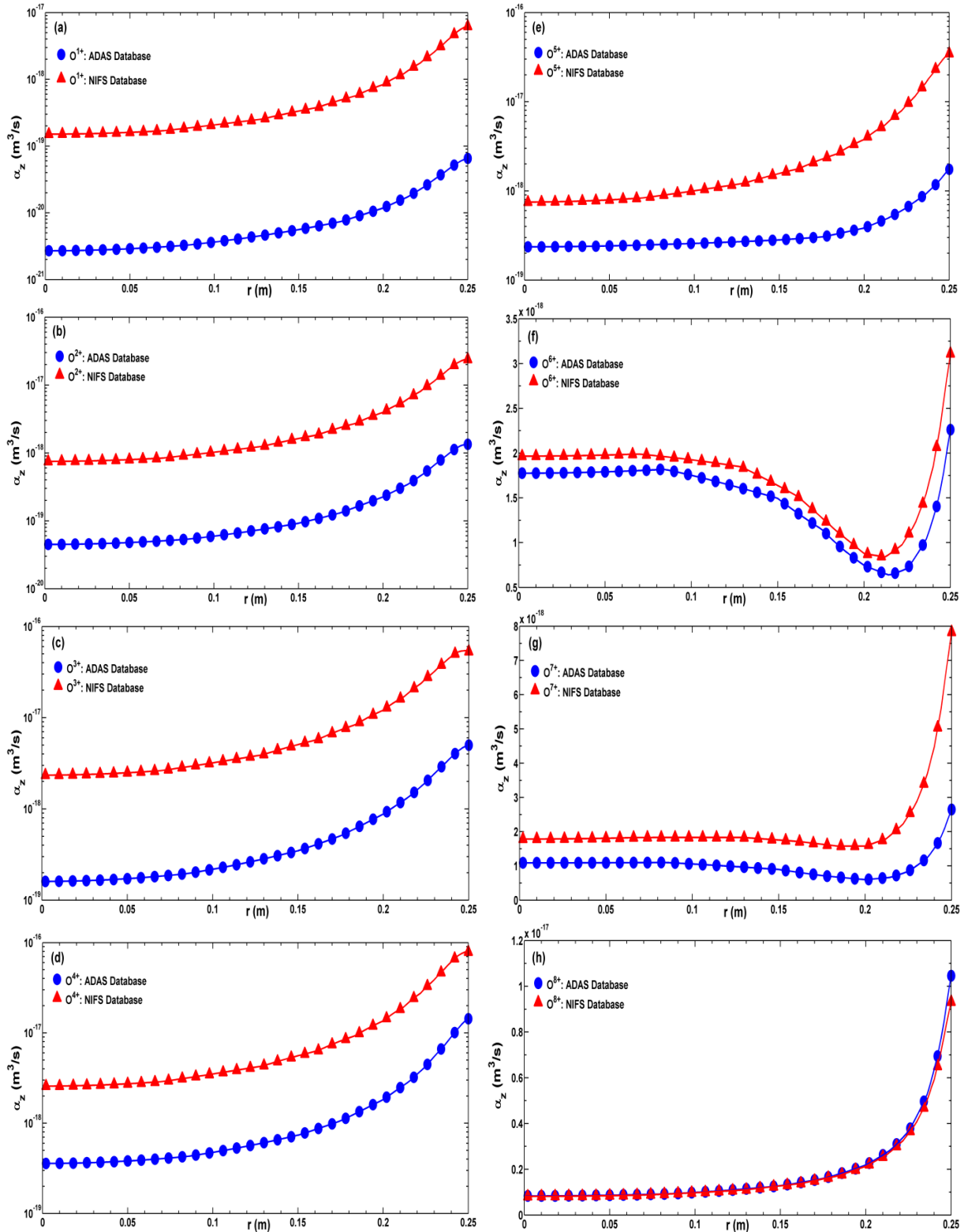
Fig. 8   Recombination Rate Coefficients α_z (m^3/s) of (a) O^{1+}, (b) O^{2+}, (c) O^{3+}, (d) O^{4+}, (e) O^{5+}, (f) O^{6+}, (g) O^{7+}, (h) O^{8+} ion with respect to radius r (m) from the ADAS and NIFS databases for the plasma parameters of Aditya tokamak.

affect the number density distribution of oxygen ions for the plasma parameters of the Aditya tokamak.

The number density profiles of O^{4+} ion shown in Fig. 9 (d) are further used, along with PECs from the

ADAS and NIFS databases (Eq. (4)), to determine their respective emissivities for the 650.024 nm transition of O^{4+} ion. Figures 10 (a), (b) describe the comparison between experimental emissivity data, the modelled Gaussian emis-
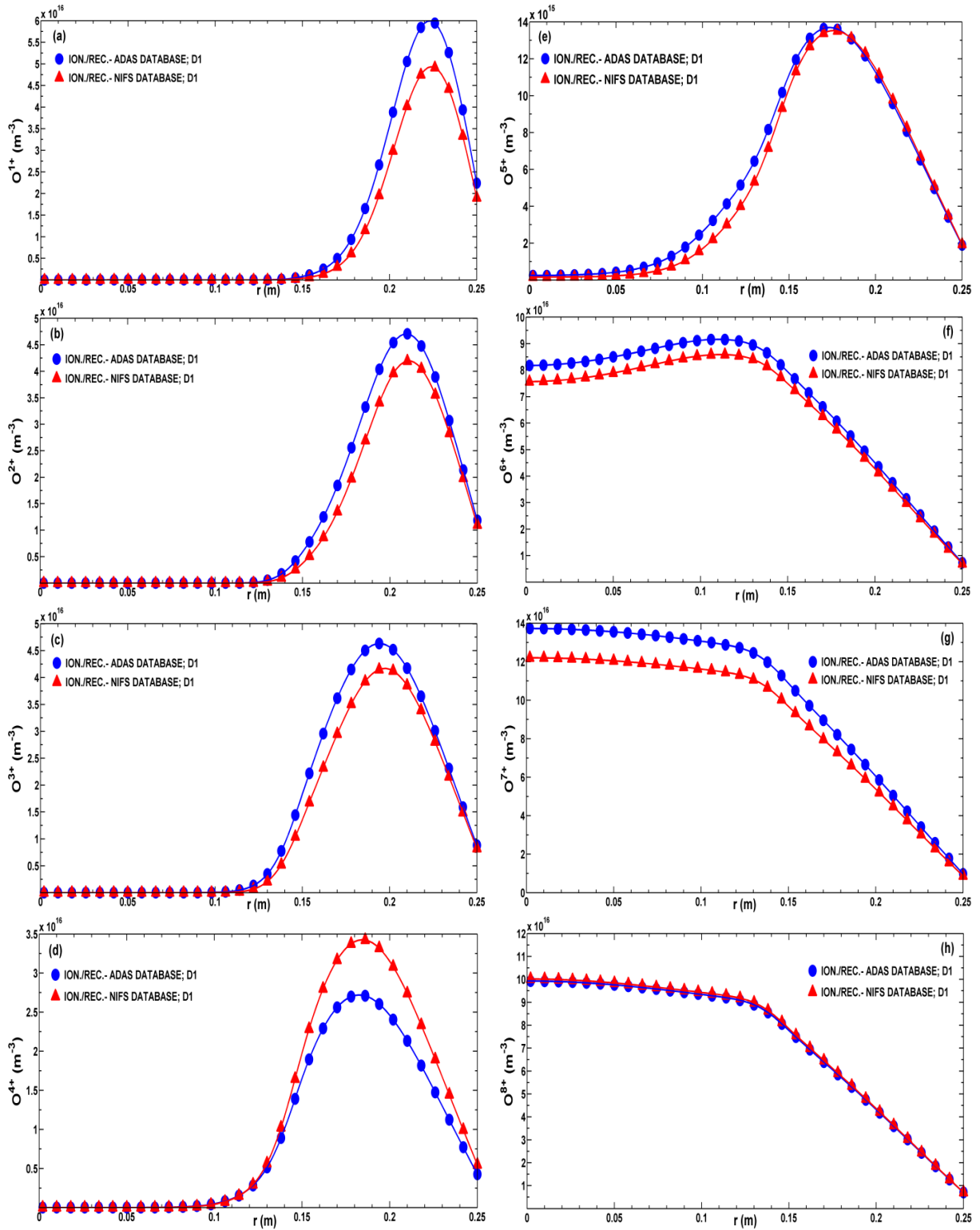
Fig. 9   Number density distribution (m^{-3}) of (a) O^{1+}, (b) O^{2+}, (c) O^{3+}, (d) O^{4+}, (e) O^{5+}, (f) O^{6+}, (g) O^{7+}, (h) O^{8+} ion with respect to radius r (m) using ionization S$_z$ (m^3/s) and recombination α_z (m^3/s) rate coefficients from the ADAS and NIFS databases and with same diffusivity D (m^2/s) profile for the two (ion./rec.) databases.

sivity profile, the calculated (semi-implicit) emissivities obtained using the O^{4+} number density profiles shown in Fig. 9 (d) and the PECs shown in Fig. 4 (a).

The 'Goodness of Fit' between the calculated

(ION./REC.+PEC) NIFS and the Gaussian emissivity is obtained as 96.37%.   The impurity diffusivity profile 'D1' as mentioned in Figs. 10 (a) - (b) represents the profile shown in Fig. 3. Table 7 compares between the experimen-

Table 6   Difference between the peaks value of oxygen ion number densities calculated using the semi-implicit numerical method with ionization and recombination rate coefficients from the ADAS and NIFS databases (with D profile: D1).

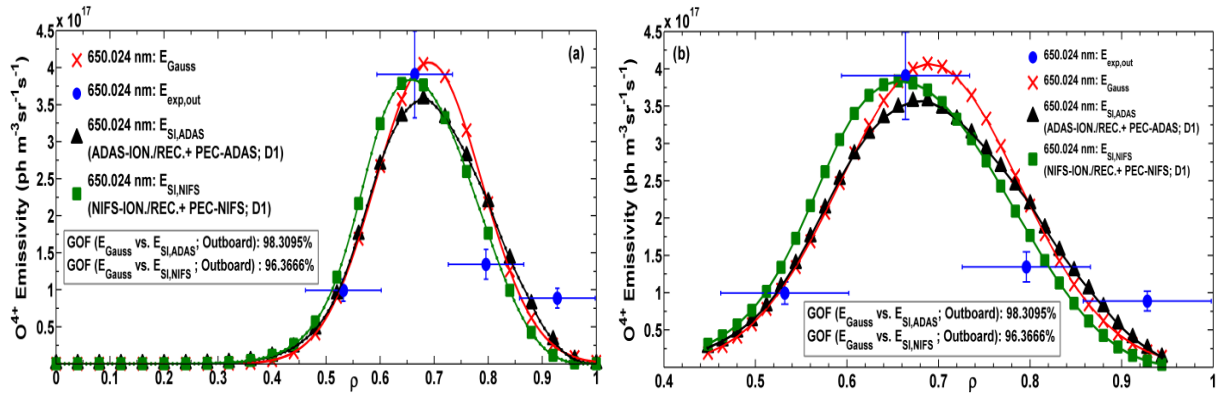| IONS	ADAS (ION. / REC.) PEAK VALUE OF NUMBER DENSITY (m⁻³) I	NIFS (ION. / REC.) PEAK VALUE OF NUMBER DENSITY (m⁻³) II	% DEVIATION [(I −II)/I] %
O^{1+}	5.9945E+16	4.9366E+16	17.649%
O^{2+}	4.7091E+16	4.1970E+16	10.874%
O^{3+}	4.6336E+16	4.1704E+16	9.997%
O^{4+}	2.7206E+16	3.4275E+16	25.980%
O^{5+}	1.3699E+16	1.3533E+16	1.211%
O^{6+}	9.1641E+16	8.5910E+16	6.253%
O^{7+}	1.3732E+17	1.2211E+17	11.074%
O^{8+}	9.9301E+16	1.0020E+17	0.902%

Fig. 10   Experimental emissivity, Gaussian emissivity and Calculated (semi-implicit) emissivities with ADAS (ION./REC.) and PEC-ADAS and with NIFS (ION./REC.) and PEC-NIFS for (a) outboard section, (b) ROI-outboard with respect to normalized radius ρ for 650.024 nm transition of O^{4+} ion (D profile: D1).

Table 7   Comparison between the experimental, modelled (Gaussian) and calculated (semi-implicit; with NIFS ION./REC. data and PEC-NIFS) emissivities of O^{4+} ion (650.024 nm transition) at four radial points of measurement in Aditya plasma (with D profile: D1).

ρ	$E_{exp, out}$	ρ_{cal}	E_{Gauss}	% deviation	$E_{SI, NIFS}$	% deviation
-	(ph m⁻³ sr⁻¹ s⁻¹)	-	(ph m⁻³ sr⁻¹ s⁻¹)	-	(ph m⁻³ sr⁻¹ s⁻¹)	-
0.928	8.868E+16	0.928	2.133E+16	75.95%	8.397E+15	90.53%
0.796	1.344E+17	0.792	2.368E+17	76.26%	1.927E+17	43.42%
0.664	3.907E+17	0.664	3.930E+17	0.58%	3.833E+17	1.91%
0.532	9.941E+16	0.528	1.038E+17	4.44%	1.340E+17	34.75%

tal emissivity values and the Gaussian and calculated O^{4+} emissivities at the four radial points of measurement in the outboard section of Aditya plasma.

Although the calculated emissivity profile, generated with number density from the NIFS ION./REC. data and

with the PEC-NIFS, is in good agreement with the Gaussian emissivity profile (GOF: 96.37%); yet the % deviation between the $E_{SI, NIFS}$ and $E_{exp, out}$ in Table 7 shows that a separate O^{4+} (650.024 nm) emissivity profile that would be in better agreement with the experimental emissivity
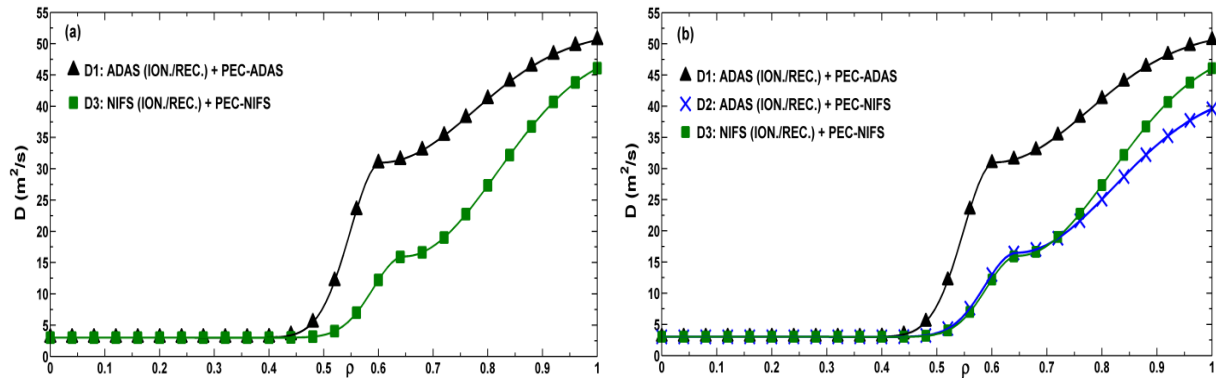
Fig. 11 Diffusivity D (m^2/s) profiles of impurity ion with respect to normalized plasma radius ρ for (a) ADAS ION./REC. data with PEC-ADAS and NIFS ION./REC. data with PEC-NIFS cases, (b) ADAS ION./REC. data with PEC-ADAS, ADAS ION./REC. data with PEC-NIFS and NIFS ION./REC. data with PEC-NIFS cases.

data is necessary. A separate impurity diffusivity profile is hence generated using Eq. (6d) where the values of various terms are as follows: $r_o = r_{LCFS} = 0.25$ m; $D_0 = 3.0$ m^2/s; $D_m = 16.0$ m^2/s; $D_a = 50.0$ m^2/s; $p_1 = 6.0$E-02 m; $p_2 = 2.0$E-02 m; $p_m = 0.647$ and $r_m = p_m \times r_{LCFS} = 0.1618$ m respectively. The newly generated diffusivity profile is represented as D3 in Figs. 11 (a), (b) respectively.

Figure 11 (b) shows a comparison between the diffusivity profiles used in three separate cases considered in present study. The profile D1 represents the impurity diffusivity values used for calculating the oxygen ion number densities when the ionization and recombination rate coefficients from the ADAS database has been used and the emissivity profile due to 650.024 nm transition is determined using the PECs from ADAS database (Fig. 3). The profile D2 represents the impurity diffusivity values used for calculating the oxygen ion number densities when the ionization and recombination rate coefficients from the ADAS database has been used and the emissivity profile due to 650.024 nm transition is determined using the PECs from NIFS database (Fig. 5 (a)). The third profile D3 represents the impurity diffusivity values used for calculating the oxygen ion number densities when the ionization and recombination rate coefficients from the NIFS database has been used and the emissivity profile due to 650.024 nm transition is determined using the PECs from NIFS database.

Figures 12 (a) - (h) describe the number density distribution of oxygen ions when the ionization rate coefficient and recombination rate coefficient data from the two separate (ADAS and NIFS) databases are used. The diffusivity profile of oxygen ions used in case of ADAS (ION./REC.) database is D1 and corresponding to NIFS (ION./REC.) database is D3. The mesh size and time step used for the semi-implicit numerical method in case of NIFS (ION./REC.) data with D3 profile are $\Delta r = 2$E-03 m and $\Delta t = 1.25$E-08 s respectively. Table 8 further describes the % deviation in the peak value of the number densities of oxygen ions shown in Figs. 12 (a) - (h) respectively. A

major change in the number densities of the oxygen ions with change in the impurity diffusivity profile from D1 to D3 is observed from the % deviation in Table 8.

The emissivity profile (650.024 nm) using the O^{4+} NIFS (ION./ REC.) number density shown in Fig. 12 (d) along with the PECs from the NIFS database (Fig. 4 (a)) is shown in Figs. 13 (a), (b). The 'Goodness of Fit' between the calculated (ION./REC.+PEC) NIFS emissivity and the Gaussian emissivity is obtained as 99.71% in present study.

Table 9 compares between the experimental emissivity values and the modelled (Gaussian) and calculated O^{4+} (650.024 nm) emissivities at four radial points of measurement in the outboard section of Aditya plasma for the present case (D3). The % deviation between $E_{SI, NIFS}$ and $E_{exp, out}$ in Table 9 show the emissivities are in good agreement with each other.

The following comparisons can be drawn based on the aforementioned observations:

1. A comparison between Figs. 9 (a) - (h) and 12 (a) - (h) and between Figs. 10 (a) and 13 (a) show that although a change in the ionization and recombination database does not affect the number density profiles of the oxygen ions; yet the O^{4+} (650.024 nm) NIFS emissivity profile in Fig. 10 (a) do not satisfactorily match with the experimental emissivity data. The O^{4+} NIFS (ION./REC.+PEC) emissivity profiles are in better agreement with experimental emissivity data (Fig. 13 (a)) when a separate impurity diffusivity profile (D3) is considered. The use of D3 as impurity diffusivity profile however leads to a significant difference in the number density profiles of oxygen ions (Fig. 12).

2. The impurity diffusivity profiles, D2 and D3 (Fig. 11 (b)), that yields the number density and consequently the O^{4+} emissivity for ADAS (ION./REC.) data with PEC-NIFS and NIFS (ION./REC.) data with PEC-NIFS (as well) respectively are similar in magnitude with a certain deviation between them only to-
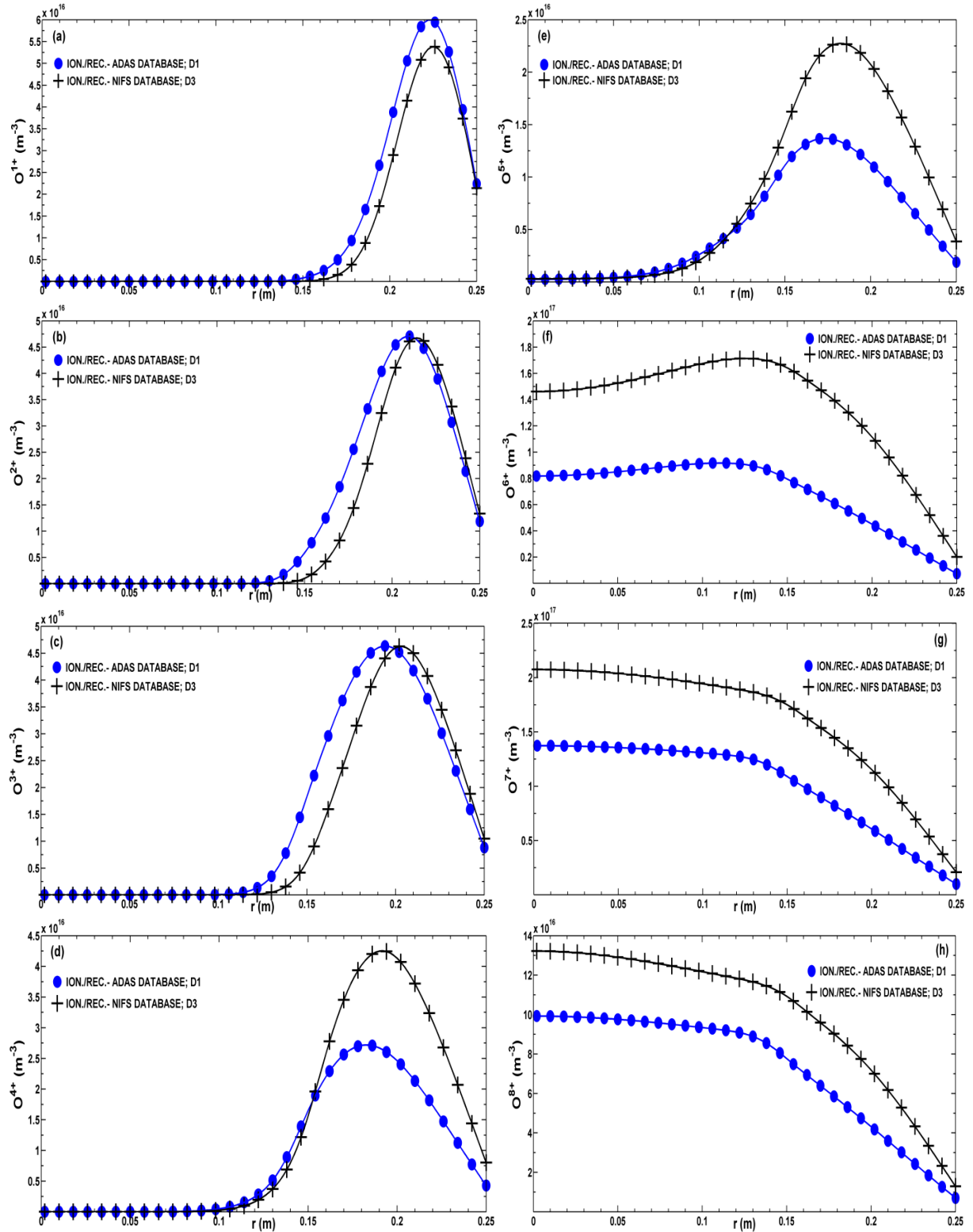
Fig. 12 Number density distribution (m^{-3}) of (a) O^{1+}, (b) O^{2+}, (c) O^{3+}, (d) O^{4+}, (e) O^{5+}, (f) O^{6+}, (g) O^{7+}, (h) O^{8+} ion with respect to radius r (m) using ionization S$_z$ (m^3/s) and recombination α_z (m^3/s) rate coefficients from the ADAS and NIFS databases and with separate diffusivity D (m^2/s) profiles for the two (ion./rec.) databases.

wards the plasma edge. The two profiles are, however, prominently different from the diffusivity profile D1 used to obtain O^{4+} emissivity in case of ADAS (ION./REC.) data with PEC-ADAS database.

The above comparisons are a direct consequence of the difference in the Photon Emissivity Coefficients between the ADAS and NIFS database derived based on the plasma parameters of Aditya tokamak. The comparisons

Table 8   Difference between peaks value of number densities calculated using semi-implicit numerical method with ionization and recombination rate coefficients from ADAS and NIFS databases (with D1 and D3).

IONS	ADAS (ION. / REC.) PEAK VALUE OF NUMBER DENSITY (m⁻³) I	NIFS (ION. / REC.) PEAK VALUE OF NUMBER DENSITY (m⁻³) II	% DEVIATION [(I −II)/I] %
O^{1+}	5.9945E+16	5.3795E+16	10.259%
O^{2+}	4.7091E+16	4.6758E+16	0.707%
O^{3+}	4.6336E+16	4.6254E+16	0.177%
O^{4+}	2.7206E+16	4.2543E+16	56.372%
O^{5+}	1.3699E+16	2.2752E+16	66.084%
O^{6+}	9.1641E+16	1.7136E+17	86.993%
O^{7+}	1.3732E+17	2.0743E+17	51.056%
O^{8+}	9.9301E+16	1.3222E+17	33.154%

Table 9   Comparison between experimental, modelled (Gaussian) and calculated (semi-implicit; with NIFS ION./REC. data and PEC-NIFS) emissivities of O^{4+} ion (650.024 nm transition) at four radial points of measurement in Aditya plasma (with D3 profile).

ρ	$E_{exp, out}$	ρ_{cal}	E_{Gauss}	% deviation	$E_{SI, NIFS}$	% deviation
-	(ph m⁻³ sr⁻¹ s⁻¹)	-	(ph m⁻³ sr⁻¹ s⁻¹)	-	(ph m⁻³ sr⁻¹ s⁻¹)	-
0.928	8.868E+16	0.928	2.133E+16	75.95%	1.198E+16	86.49%
0.796	1.344E+17	0.792	2.368E+17	76.26%	2.507E+17	86.54%
0.664	3.907E+17	0.664	3.930E+17	0.58%	4.003E+17	2.45%
0.532	9.941E+16	0.528	1.038E+17	4.44%	8.797E+16	11.51%
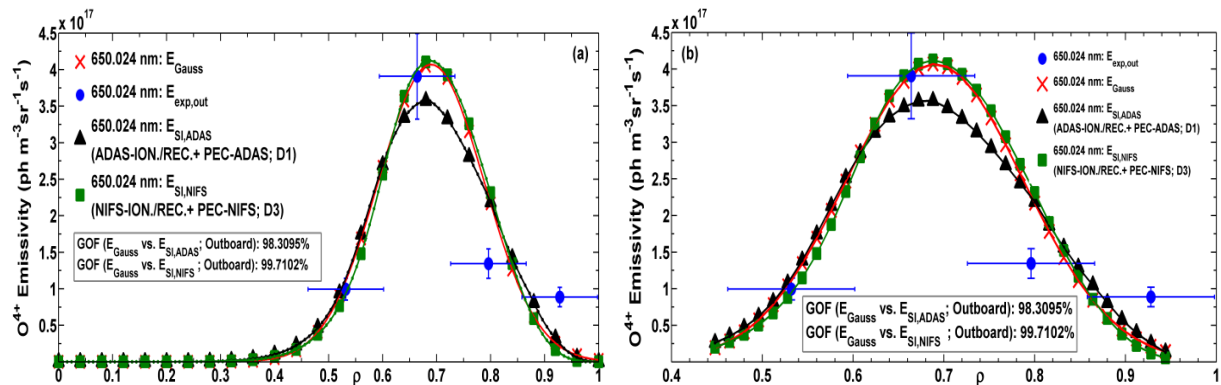
Fig. 13   Experimental emissivity data, Gaussian emissivity model and Calculated (semi-implicit) emissivities with ADAS (ION./REC.) and PEC-ADAS and with NIFS (ION./REC.) and PEC-NIFS for (a) outboard section, (b) ROI-outboard with respect to normalized radius ρ for 650.024 nm transition of O^{4+} ion (D profiles: D1 & D3).

further enunciate the impact of the change in PECs from ADAS to NIFS database is significant over the impurity diffusivity profile than the change in ionization and recombination rate coefficients from ADAS to NIFS database.

4. Summary

✓ The chord-integrated brightness in the outboard section of Aditya plasma for 650.024 nm O^{4+} transition has been measured experimentally. The O^{4+} emissivity over the radial points of measurement is determined using Abel-like matrix inversion over the chord-integrated brightness and the poloidal asymmetry in emissivity has also been considered. The uncertainty associated with each experimental emissivity data is ~ ±15%.

✓ A semi-implicit numerical scheme has been developed for solving the radial impurity transport equation in tokamak plasma. The present study compares the emissivity due to 650.024 nm characteristic transition of O^{4+} ion obtained using O^{4+} number density calculated using the semi-implicit numerical method with experimental emissivity data in the outboard section of Aditya plasma.

✓ Gaussian profiles have been generated to fit the experimental emissivity data best describing the O^{4+} (650.024 nm) emissivity at all radii in the outboard section of Aditya tokamak. The O^{4+} emissivity calculated using the semi-implicit method applied is compared with the Gaussian emissivity model such that the 'goodness of fit' between them remains above 95%.

✓ The O^{4+} emissivity is calculated using the Photon Emissivity Coefficients (PECs) from two separate databases namely the ADAS and NIFS database. The difference between the PEC coefficient profiles of the 650.024 nm O^{4+} transition obtained from the ADAS and NIFS database is more extensive (in orders of 10) towards the plasma edge than towards the plasma centre especially for $\rho \geq 0.6$.

✓ The excitation rate coefficients based on which the PECs of the 650.024 nm characteristic transition of the O^{4+} ion are calculated are different for the ADAS and NIFS databases. A modification in the impurity diffusivity profile while using PEC-NIFS is required to match its calculated O^{4+} emissivity with experiment emissivity data in Aditya plasma.

✓ A change in the ionization and recombination rate coefficients from the ADAS to NIFS database, derived based on the plasma parameters of Aditya tokamak, keeping all input parameters to the semi-implicit numerical method same; does not affect the number density distribution of the oxygen ions in the Aditya plasma.

5. Conclusion

A change in ionization/recombination data from ADAS (ION./REC.) to NIFS (ION./REC.) does not have an impact of the same magnitude on the O^{4+} emissivity and therefore on the impurity transport coefficient (Diffusivity in the present study) as much as the change in PECs from PEC-ADAS to PEC-NIFS database has on the same. The Photon Emissivity Coefficients (PECs) of the ADAS and NIFS database differ based on the atomic and molecular processes considered while calculating them. Impurity accumulation towards the plasma core of a tokamak is a serious concern in thermonuclear fusion research. The knowledge of impurity diffusivities and their radial profiles is hence very important. The impurity diffusivities further provide, the much needed for identifying processes, responsible in the impurity transport in tokamaks as classical

transport theory fails to explain the impurity concentration and distribution inside tokamak plasma. Large diffusivity values observed in tokamaks points towards the fluctuation induced transport of impurities. The values of diffusivities estimated using ADAS database as reported by M.B. Chowdhuri et al., [9] shows that a combination of resistive ballooning modes and ion temperature gradient modes may be governing the impurity transport in Aditya tokamak. Our estimates using ADAS database also confirms the same, however, when the NIFS database is used, relatively lower values of diffusivities are obtained over the entire analysed plasma region ($\rho \sim 0.5$ - 1). The values of diffusivities obtained using NIFS database point out that either the resistive ballooning modes or the ion temperature gradient modes seems to be responsible for the oxygen (impurity) transport. Although the existing databases provide the all-important data (atomic and molecular) that assists in gathering the required insights to the processes occurring inside the plasma; yet the present study suggests a possibility of iterations through the comparison of databases.

[1] C. Breton, C. De Michelis and M. Mattioli, Nucl. Fusion **16 (6)**, 891 (1976).

[2] D. Post, J. Abdallah, R.E.H. Clark and N. Putvinskaya, Phys. Plasmas **2**, 2328 (1995).

[3] A. Kirschner, V. Philipps, J. Winter and U. Kögler, Nucl. Fusion **40 (5)**, 989 (2000).

[4] P.C. Stangeby, *The Plasma Boundary of Magnetic Fusion Devices* (IOP Publishing Ltd., Bristol, 2000).

[5] I. Condrea, E. Haddad, B.C. Gregory and G. Abel, Phys. Plasmas **7**, 3641 (2000).

[6] J. Ghosh, R.C. Elton, H.R. Griem, A. Case, A.W. DeSilva, R.F. Ellis, A. Hassam, R. Lunsford and C. Teodorescu, Phys. Plasmas **13**, 022503 (2006).

[7] M. Goswami, P. Munshi, A. Saxena, M. Kumar and A. Kumar, Fusion Eng. Des. **89(11)**, 2659 (2014).

[8] S. Banerjee, V. Kumar, M.B. Chowdhuri, J. Ghosh, R.

Manchanda, K.M. Patel and P. Vasu, Measurement Sci. Technol. **19**, 045603 (2008).

[9] M.B. Chowdhuri, J. Ghosh, S. Banerjee, R. Dey, R. Manchanda, V. Kumar, P. Vasu, K.M. Patel, P.K. Atrey, Y. Shankara Joisa, C.V.S. Rao, R.L. Tanna, D. Raju, P.K. Chattopadhyay, R. Jha, C.N. Gupta, S.B. Bhatt, Y.C. Saxena and the Aditya Team, Nucl. Fusion **53**, 023006 (2013).

[10] W. Horton and W. Rowan, Phys. Plasmas **1**, 901 (1994).

[11] S. Sudo, Plasma Phys. Control. Fusion **58**, 043001 (2016).

[12] K. Lackner, K. Behringer, W. Engelhardt and R. Wunderlich, Zeitschrift für Naturforschung **37a(5)**, 931 (1982).

[13] J. Wesson, *Tokamaks*, 3rd Edition (Clarendon Press, Oxford, 2004).

[14] A. Bhattacharya, P. Munshi, J. Ghosh and M.B. Chowdhuri, J. Fusion Energy **37 (5)**, 211 (2018).

[15] 2019, HPC2013, 'High Performance Computing system', Indian Institute of Technology Kanpur, https://www.iitk.ac.in/ccnew/index.php/hpc (as on 05. 01. 2019).

[16] R. Dey, J. Ghosh, M.B. Chowdhuri, R. Manchanda, S. Banerjee, N. Ramaiya, D. Sharma, R. Srinivasan, D.P. Stotler and Aditya Team, Nucl. Fusion **57**, 086003 (2017).

[17] TFR group, Association Euratom - CEA sur la fusion, Département de recherches sur la fusion controlée, Centre d'études nucléaires, Fontenay-aux-Roses, France, Nucl. Fusion **22**, 1173 (1982).

[18] 2019, http://open.adas.ac.uk/ 'Effective Ionization Rate Coefficients', 'Effective Recombination Rate Coefficients', Oxygen (as on 05.01.2019).

[19] R. Dux, 'Impurity Transport in tokamak plasma' – STRAHL manual, IPP 10/27 Garching (2005).

[20] G. Fussman, A.R. Field, A. Kallenbach, K. Kreiger, K.-H. Steuer and the ASDEX team, Plasma Phys. Control. Fusion **33(13)**, 1677 (1991).

[21] R. Guirlet, C. Giroud, T. Parisot, M.E. Puiatti, C. Bourdelle, L. Carraro, N. Dubuit, X. Garbet and P.R. Thomas, Plasma Phys. Control. Fusion **48**, B63 (2006).

[22] S.P. Hirshman and D.J. Sigmar, Nucl. Fusion **21(9)**, 1079 (1981).

[23] H. Nozato, S. Morita, M. Goto, Y. Takase, A. Ejiri, T. Amano, K. Tanaka, S. Inagaki and LHD experimental group, Phys. Plasmas **11(5)**, 1920 (2004).

[24] R. Dux, A.G. Peeters, A. Gude, A. Kallenbach, R. Neu and ASDEX Upgrade Team, Nucl. Fusion **39(11)**, 1509 (1999).

[25] 2019, ADAS Database, 'Photon Emissivity Coefficients', http://open.adas.ac.uk/adf15 (as on 05.01.2019).

[26] 2019, NIFS Database, 'AMDIS IONIZATION', https://dbshino.nifs.ac.jp/nifsdb/amdis_ion/top 'AMDIS RECOMBINATION', https://dbshino.nifs.ac.jp/nifsdb/amdis_rec/top (as on 05.01.2019).